Ad Hoc Networks 12 (2014) 100–114

Contents lists available at SciVerse ScienceDirect

Ad Hoc Networks

journal homepage: www.elsevier.com/locate/adhoc

Low-dimensional signal-strength fingerprint-based positioning in wireless LANs

Dimitris Milioris [a,b,c], George Tzagkarakis [d], Artemis Papakonstantinou [a,e], Maria Papadopouli [a,e,f,*], Panagiotis Tsakalides [a,e]

[a] Department of Computer Science, University of Crete, P.O.Box 2208, Heraklion, Crete, GR–714 09, Greece
[b] Département d' Informatique, Université Paris-Sud XI, France
[c] INRIA – Rocquencourt, Paris, France
[d] CEA, IRFU/SEDI-LCS, Centre de Saclay, France
[e] Institute of Computer Science – FORTH, Crete, Greece
[f] School of Electrical Engineering, KTH Royal Institute of Technology, Stockholm, Sweden

ARTICLE INFO

Article history:
Received 3 June 2011
Received in revised form 2 November 2011
Accepted 6 December 2011
Available online 24 December 2011

Keywords:
Compressive sensing
Sparse representation
Multivariate Gaussian model
Kullback–Leibler divergence
RSSI measurements
Localization

ABSTRACT

Accurate location awareness is of paramount importance in most ubiquitous and pervasive computing applications. Numerous solutions for indoor localization based on IEEE802.11, bluetooth, ultrasonic and vision technologies have been proposed. This paper introduces a suite of novel indoor positioning techniques utilizing signal-strength (SS) fingerprints collected from access points (APs). Our first approach employs a statistical representation of the received SS measurements by means of a multivariate Gaussian model by considering a discretized grid-like form of the indoor environment and by computing probability distribution signatures at each cell of the grid. At run time, the system compares the signature at the unknown position with the signature of each cell by using the Kullback–Leibler Divergence (KLD) between their corresponding probability densities. Our second approach applies compressive sensing (CS) to perform sparsity-based accurate indoor localization, while reducing significantly the amount of information transmitted from a wireless device, possessing limited power, storage, and processing capabilities, to a central server. The performance evaluation which was conducted at the premises of a research laboratory and an aquarium under real-life conditions, reveals that the proposed statistical fingerprinting and CS-based localization techniques achieve a substantial localization accuracy.

1. Introduction

Location-sensing has been impelled by the emergence of location-based services in the transportation industry, emergency situations for disaster relief, the entertainment industry, and assistive technologies in the medical community. Location-sensing systems can be classified according to their dependency on and/or use of (a) specialized infrastructure and hardware, (b) signal modalities, (c) training, (d) methodology and/or use of models for estimating distances, orientation, and position, (e) the coordination system (absolute or relative), scale, and location description, (f) localized or remote computation, their mechanisms for device identification, classification, and recognition, and their accuracy and precision requirements. The distance can be estimated using time-of-arrival (*e.g.,* GPS, PinPoint [1]) or signal-strength measurements, if the velocity of the signal and a signal attenuation model for the environment can be accurately estimated, respectively. Positioning systems may employ different modalities, such as, IEEE802.11 (*e.g.,* Radar [2,3], Ubisense, Ekahau [4]), infrared (*e.g.,* Active Badge [5]), ultrasonic (*e.g.,* Cricket [6,7], Active

* Corresponding author at: Department of Computer Science, University of Crete, P.O.Box 2208, Heraklion, Crete, GR–714 09, Greece.
E-mail address: mgp@ics.forth.gr (M. Papadopouli) .

1570-8705/$ - see front matter © 2012 Published by Elsevier B.V.
doi:10.1016/j.adhoc.2011.12.006

Bat), Bluetooth [3,8–11], 4G [12], vision (*e.g., EasyLiving* project), and physical contact with pressure (*e.g., Smart Floor*), touch sensors or capacitive detectors. They may also combine multiple modalities to improve the localization, such as optical, acoustic and motion attributes (*e.g.,* SurroundSense [13]).

The popularity of IEEE802.11 infrastructures, their low deployment cost, and the advantages of using them for both communication and positioning, make them an attractive choice. Most of the signal-strength based localization systems can be classified into the following two categories, namely *signature- or map*-based and *distance-prediction*-based techniques. The first type creates a signal-strength signature or map of the physical space during a training phase and compares it with the signature generated at runtime (at the unknown position) [2,14,15]. To build such signatures, signal-strength data is gathered from beacons received from APs. During a training phase, such measurements are collected at various predefined positions (of the map) and signatures are generated that associate the corresponding positions of the physical space with statistical measurements based on signal-strength values acquired at those positions. Such maps can be formed with data from different sources or signal modalities to improve location-sensing [3,6]. The distance-prediction-based techniques use the signal-strength values and radio-propagation models to predict the distance of a wireless client from an AP (or any landmark) or even between two wireless clients (peers) with estimated position (such as CLS [16]). In situations where a deployment of a wireless infrastructure may not be feasible, positioning mechanisms may exploit cooperation by enabling devices to share positioning estimates [1,16–22]. A survey of positioning systems can be found in [23].

In this paper, first we build on our earlier work on CLS [16,20], which generates statistical-based fingerprints using the *received signal-strength* (RSSI) measurements from an IEEE802.11 infrastructure. The vast majority of current fingerprint positioning methods does not take into account the interdependencies among the RSSI measurements at a certain position from the various APs. These interdependencies provide important information about the geometry of the environment and can be quantified using the second-order spatial correlations among the measurements. Hence, the employment of multi-dimensional distributions is expected to provide a more accurate representation of the RSSI signatures, leading to improved positioning performance. Simple models whose second-order statistics can be accurately and easily estimated could be used in practice. In particular, a multivariate Gaussian-based approach is employed to take into consideration the statistics of the RSSI measurements not only from each distinct AP but also the interplay (covariance) of measurements collected from pairs of APs. The signature comparison and position estimation is based on the Kullback–Leibler divergence (KLD): the cell corresponding to the minimum KLD is reported as the estimated position. This approach is generalized by applying it iteratively in different spatial scales.

The difficult to predict nature of the RSSI measurements, due to the impact of transient phenomena on the RSSI values, impels for extensive training, which increases the overhead of the fingerprint-based positioning systems: a larger training set and more sophisticated algorithms are often employed to capture the dynamic complex nature of the RSSI measurements. On the other hand, the inherent sparse nature of the localization of a mobile device in the physical space (since it can be placed at a single position of a discretized grid-like form of the environment) motivates the use of the recently introduced theory of *compressive sensing* (CS) [24,25] for target localization [26]. CS states that signals which are sparse in a suitable transform basis can be recovered from a highly reduced number of incoherent random projections. Hence, the CS-based approach comes as an evolution to the traditional methods dominated by the well-established Nyquist–Shannon sampling theory, and consequently it could be exploited in the design of efficient localization systems characterized by limited resources.

In a recent work [27], a CS-based indoor localization method was introduced based on RSSI measurements. In particular, the location estimation algorithm is carried out on the mobile device by using the average RSSI values in order to construct the transform basis. The sparsity-based CS localization algorithm proposed in this paper differs from the work in [27] in several aspects. In contrast to [27], where the estimation is performed by the wireless device with the potentially limited resources, in our proposed algorithm the computational burden can be assigned to a central node (fusion center), where increased storage and processing resources are available. Unlike in [27] that uses the average RSSI values, the proposed CS approach is applied directly on the raw RSSI measurements, thus exploiting their time-varying behavior. Then, the estimation of the unknown position is performed by solving a constraint optimization problem for reconstructing a sparse vector with its coordinates being "1" or "0" depending on whether the mobile device is placed or not at the corresponding cell.

This paper makes the following contributions:

1. It proposes and evaluates a novel fingerprinting approach that exploits the spatial correlations of signal-strength measurements collected from various wireless APs based on a *multivariate Gaussian* model.
2. It introduces a novel localization approach that applies *compressive sensing* (CS), which can achieve an increased accuracy in the position estimation, while reducing the communication overhead required for the exchange of measurements, and thus, becoming more appropriate for energy-constrained devices.
3. It performs a comparative performance analysis of various signal-strength fingerprinting methods in the premises of a research laboratory and an aquarium under different conditions.

The paper is organized as follows: Section 2 presents recently introduced statistical signal-strength signature techniques, along with the proposed statistical approach based on the use of multivariate Gaussian distributions for modelling the statistics of the RSSI measurements. In Section 3, the main principles of CS are introduced and the proposed CS-based localization method is analyzed in detail. Section 4

presents a comparative performance evaluation of these techniques in the premises of the Telecommunications and Networks Lab (TNL) at ICS-FORTH as well as in the Cretaquarium. Section 5 overviews related positioning systems for mobile computing, while Section 6 summarizes our main results and provides directions for future work.

2. Statistical fingerprint methods

A wireless device that listens to a channel receives the beacons sent by APs (at that channel) periodically and records their RSSI values. Typically wireless devices that run fingerprint-based positioning systems acquire such measurements at various positions in a given physical space (with a deployment of wireless APs) and generate fingerprints for these positions applying various statistical metrics (*e.g.,* confidence intervals, percentiles, empirical distributions or the parameters of a theoretical distribution) on the collected measurements. The physical space is often represented as a grid of cells with fixed size and well-known coordinates. During a training phase, at known positions of the physical space, such measurements are collected by a wireless client (*training measurements*). At each position, the wireless client scans all the available channels and listens for beacons from APs. During the runtime phase, the system also records the RSSI values from the received beacons (*runtime measurements*). As in the case of training, the wireless client scans all the available channels.

A statistical-based signature is constructed for each cell of the grid using the signal-strength measurements collected during the training phase (*training signature*). Similarly, applying the same statistical method, at runtime, a statistical-based signature is also generated using the runtime measurements collected at the location of the device (at an unknown cell) on-the-fly (*runtime signature*). The runtime signature is then compared with all the training signatures. The *fingerprint of a cell* is a vector of training signatures with size equal to the number of APs deployed in the area. Each entry of the vector corresponds to one AP. The fingerprint of the unknown position is the corresponding vector of the runtime signatures. The cell with a training fingerprint that has the smallest distance from the runtime fingerprint is reported as the estimated position. The next paragraphs present the various methods for generating the statistical-based signatures used in this work.

2.1. Confidence intervals

In the confidence-interval approach the signature is a vector of confidence intervals, each corresponding to an AP. Each confidence interval is generated using the RSSI values of the beacons received from the corresponding AP by the mobile device. Let us denote as $[T_i^-(t), T_i^+(t)]$ the confidence interval for AP i at cell t during the training phase. The fingerprint of a cell is the vector of these confidence intervals (for all APs) at that cell. Similarly, at runtime, at the unknown position, the system records the RSSI values from a number of beacons sent by the APs and computes a confidence interval for each AP. For example, the runtime confidence interval for AP i is the $[R_i^-, R_i^+]$. The runtime fingerprint is a vector composed by all confidence intervals formed at runtime from all APs. An AP i participates in this technique by assigning a *vote (weight) for a cell t* that indicates the similarity of its training confidence interval $[T_i^-(t), T_i^+(t)]$ with the runtime confidence interval $[R_i^-, R_i^+]$ according to the following rule:

$$w(t) = \begin{cases} \frac{T_i^+(t)-R_i^-}{R_i^+-T_i^-(t)} & \text{if } T_i^-(t) < R_i^- < T_i^+(t) < R_i^+ \\ \frac{R_i^+-T_i^-(t)}{T_i^+(t)-R_i^-} & \text{if } R_i^- < T_i^-(t) < R_i^+ < T_i^+(t) \\ 1 & \text{if } R_i^- \leqslant T_i^-(t) < T_i^+(t) \leqslant R_i^+ \\ & \text{or } T_i^-(t) \leqslant R_i^- < R_i^+ \leqslant T_i^+(t) \\ 0 & \text{if } R_i^- < R_i^+ \leqslant T_i^-(t) < T_i^+(t) \\ & \text{or } T_i^-(t) < T_i^+(t) \leqslant R_i^- < R_i^+ \end{cases} \quad (1)$$

By adding these weights, the confidence-interval approach computes a weight for that cell that indicates its likelihood to be the unknown position (at which the corresponding runtime measurements were collected).

At the start of the runtime phase, each cell has a zero weight. For each cell, the training confidence interval of each AP is compared with the corresponding (for that AP) runtime confidence interval at the unknown cell c. The algorithm assigns a weight at cell c, $w(c)$, that indicates the likelihood that this cell is the position of the device. Each AP participates by assigning a vote to that cell. Specifically, the weight of that cell is increased by a specific value, as follows: In the case that the training confidence interval is included in the runtime confidence interval or the runtime confidence interval is included in the training confidence interval, the weight of that cell is increased by one. In the case of a partial overlap of these two confidence intervals, the value indicates the ratio of this overlap. The cell with the maximum weight is reported as the estimated position.

A drawback of this method, and especially of the voting assignment (as defined in (1)), is its sensitivity to the relative position of the endpoints (boundaries) of the confidence interval. Even a small displacement of an endpoint (in the runtime confidence interval relative to the training confidence interval) may affect significantly the value of the weight. Furthermore, there are cases in which two relatively distant cells may report the same maximum weight. Let us illustrate these cases with some examples. For convenience, consider the simplified scenario of a single AP and the signatures of one runtime and two training cells, $c \mapsto [R^-(c), R^+(c)]$, $t_1 \mapsto [T^-(t_1), T^+(t_1)]$, $t_2 \mapsto [T^-(t_2), T^+(t_2)]$.

- *Example 1*: Let us form the cases A and B, as shown in Fig. 1a, case A: $T^-(t_1) < R^-(c) < R^+(c) < T^+(t_1)$ case B: $T^-(t_1) < R^-(c) < T^+(t_1) < R^+(c)$ with $R^-(c) = T^+(t_1) - \epsilon$, $R^+(c) = T^+(t_1) + \epsilon$
  In case A, the rule (1) reports a weight equal to 1, while in case B the weight is equal to

$$\frac{T^+(t_1) - R^-(c)}{R^+(c) - T^-(t_1)} = \frac{T^+(t_1) - T^+(t_1) + \epsilon}{T^+(t_1) + \epsilon - T^-(t_1)} = \frac{\epsilon}{T^+(t_1) - T^-(t_1) + \epsilon}.$$

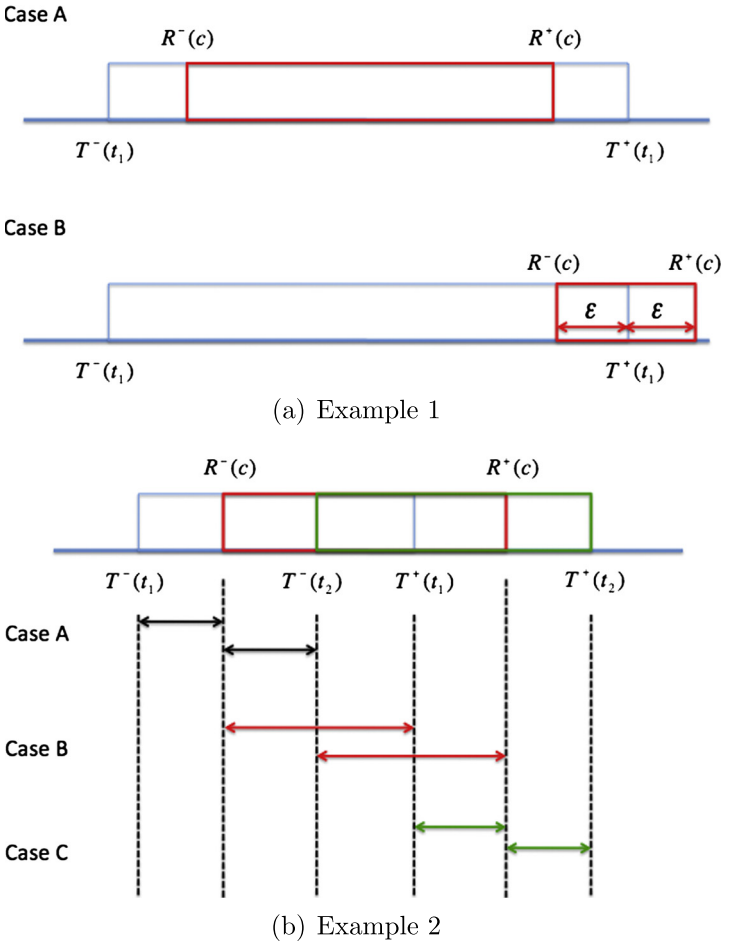

Fig. 1. Drawback of the weighting process in the confidence interval method.

For a displacement $\epsilon \to 0$, the weight in case B is equal to 0. That is, even if the unknown runtime cell c coincides with the training t_1, a small variation of the RSSI measurements may affect significantly the corresponding weight.

- *Example 2*: Let us now assume that the endpoints of the confidence intervals of the cells c, t_1 and t_2 are related as follows: $T^-(t_1) < R^-(c) < T^+(t_1) < R^+(c)$, $R^-(c) < T^-(t_2) < R^+(c) < T^+(t_2)$ with

$$|T^-(t_1) - R^-(c)| = |R^-(c) - T^-(t_2)|$$
$$|R^-(c) - T^+(t_1)| = |T^-(t_2) - R^+(c)|$$
$$|T^+(t_1) - R^+(c)| = |T^+(t_2) - R^+(c)|$$

In that case (as shown in Fig. 1b), the confidence interval method assigns the same weight to both training cells, being unable to distinguish between t_1 and t_2.

2.2. Percentiles

This approach is similar to the confidence-interval one. However, instead of using confidence intervals for constructing the fingerprints, percentiles are employed. A set of percentiles can capture more detailed information about the signal-strength distribution than a confidence interval. The weight of a cell c, $w(c)$, is computed as follows:

$$w(c) = \sum_{i=1}^{P} \sqrt{\sum_{j=1}^{n_p} (R_j^i - T_j^i(c))^2}, \quad (2)$$

where P is the number of APs, n_p the number of percentiles, R_j^i the jth percentile of runtime measurements from the ith AP and $T_j^i(c)$ the jth percentile using the training measurements from the ith AP at the cell c. The cell with the minimum weight is reported as the estimated position. In the case of the *top 5 weighted percentiles* approach, a "weighted centroid" of the five cells with the smallest weight is reported, with the weights being the normalized votes of these cells.

2.3. Empirical distribution

The signature of a cell is a vector of size equal to the number of APs that appear in both the training and runtime measurements. Each entry of a training (runtime) signature corresponds to the complete set of RSSI values collected during the training (runtime) phase, respectively.

This method creates a signature based on the set of signal-strength measurements collected at each cell from all APs. At runtime, at an unknown position, each cell is assigned a *weight* which corresponds to the *average empirical* KLD of each AP (at that cell) from the runtime measurements collected at the unknown position from the same AP. The cell with the smallest weight is reported as the position.

2.4. Multivariate Gaussian model

Unlike other fingerprint positioning approaches, the Multivariate Guassian model (MvG) aims to exploit the interdependencies among the RSSI measurements in a cell from various APs. These interdependencies may reveal information about the geometry/topology of the environment and can be quantified using the second-order spatial correlations among the measurements. According to this approach, a statistical signature is generated for each cell of the grid by modelling the acquired signal-strength measurements using a multivariate Gaussian distribution. The density function of a multivariate Gaussian in $\mathbb{R}^K$ with a mean vector $\boldsymbol{\mu}$ and covariance matrix $\boldsymbol{\Sigma}$ is given by:

$$p(\mathbf{x}|\boldsymbol{\mu},\boldsymbol{\Sigma}) = \frac{1}{(2\pi)^{K/2}|\boldsymbol{\Sigma}|^{1/2}} \exp\left(-\frac{1}{2}(\mathbf{x}-\boldsymbol{\mu})^T\boldsymbol{\Sigma}^{-1}(\mathbf{x}-\boldsymbol{\mu})\right), \tag{3}$$

where $|\boldsymbol{\Sigma}|$ is the determinant of $\boldsymbol{\Sigma}$.

Let P be the number of APs from which the mobile device receives the measurements, M be the number of measurements from each AP, and $\mathbf{S}_i = [\mathbf{y}_1, \ldots, \mathbf{y}_P]$ denote the $M \times P$ matrix for the ith cell c_i, whose jth column $\mathbf{y}_j \in \mathbb{R}^M$ contains the received signal-strength values from the jth AP. The signal-strength measurements are modelled by a multivariate Gaussian distribution due to its simplicity and the closed-form expression of the associated similarity measure (KLD). More specifically, the signature $\mathcal{S}_i$ of the ith cell is given by:

$$c_i \mapsto \mathcal{S}_i = \{\boldsymbol{\mu}_i, \boldsymbol{\Sigma}_i\}, \tag{4}$$

where $\boldsymbol{\mu}_i = [\mu_{i,1}, \ldots, \mu_{i,P}]$, with $\mu_{i,j}$ being the mean of the jth column of the measurement matrix $\mathbf{S}_i$, and $\boldsymbol{\Sigma}_i$ is the corresponding covariance matrix, with its mnth element being equal to the covariance between the mth and nth columns of $\mathbf{S}_i$. Hence, the mnth element of $\boldsymbol{\Sigma}_i$ corresponds to the *spatial correlation* between the RSSI measurements of the ith cell received from the $m-$th and nth APs. Thus, if C is the number of cells in the grid representing the physical space, during the training phase, the following set of *training* signatures (T) is generated:

$$\{\mathcal{S}_{i,T}\}_{i=1}^{C} = \{\{\boldsymbol{\mu}_{i,T}, \boldsymbol{\Sigma}_{i,T}\}\}_{i=1}^{C}. \tag{5}$$

In addition, the ith training cell, $c_{i,T}$, is also associated to a set of indices $I_{i,T}$ indicating its corresponding "active" APs, that is, the APs from which it acquires the measurements during the training phase.

During the *runtime* phase (R), we assume that the mobile user is placed at an unknown cell (c_R), whose location must be estimated. Following the approach used in the training phase, if $\mathbf{S}_R = [\mathbf{y}_{1,R}, \ldots, \mathbf{y}_{P',R}]$ is the $M' \times P'$ runtime signal-strength measurement matrix of c_R, a signature is generated as follows:

$$c_R \mapsto \mathcal{S}_R = \{\boldsymbol{\mu}_R, \boldsymbol{\Sigma}_R\}. \tag{6}$$

Notice here that in general the dimensions of the runtime measurement matrix are smaller than the dimensions of the corresponding training matrix ($M \times P$) due to the increased time constraints to collect extensive measurements during runtime. Furthermore, the set of APs operating during the training phase is *not* necessarily the same with the set of APs at runtime.

Let us denote as $I_R^{i,T}$ the set of APs from which signal-strength measurements were collected *both at runtime and training* at cell i. For the runtime (c_R) and the ith training cell ($c_{i,T}$), we extract their corresponding mean sub-vectors $\boldsymbol{\mu}_R^s$, $\boldsymbol{\mu}_{i,T}^s$ and covariance sub-matrices $\boldsymbol{\Sigma}_R^s$, $\boldsymbol{\Sigma}_{i,T}^s$ according to the indices of $I_R^{i,T}$. Finally, if $p_R(\mathbf{x}|\boldsymbol{\mu}_R^s, \boldsymbol{\Sigma}_R^s)$ and $p_{i,T}(\mathbf{x}|\boldsymbol{\mu}_{i,T}^s, \boldsymbol{\Sigma}_{i,T}^s)$ denote the multivariate Gaussian densities of c_R and $c_{i,T}$, respectively, their KLD is given by the following closed-form expression:

$$D(p_R\|p_{i,T}) = \frac{1}{2}\Big((\boldsymbol{\mu}_{i,T}^s - \boldsymbol{\mu}_R^s)^T(\boldsymbol{\Sigma}_{i,T}^s)^{-1}(\boldsymbol{\mu}_{i,T}^s - \boldsymbol{\mu}_R^s) + tr\Big(\boldsymbol{\Sigma}_R^s(\boldsymbol{\Sigma}_{i,T}^s)^{-1} - \mathbf{I}\Big) - \ln|\boldsymbol{\Sigma}_R^s(\boldsymbol{\Sigma}_{i,T}^s)^{-1}|\Big), \tag{7}$$

where $tr(\cdot)$ denotes the trace of a matrix (sum of its diagonal elements) and $\mathbf{I}$ is the identity matrix. KLD is a (non-symmetric) measure of the difference between two probability distributions, well-established and widely-used in probability and information theory. The estimated location $[x_R^*, y_R^*]$ is given by the coordinates of the i^*th cell which minimizes (7), that is,

$$i^* = \arg\min_{i=1,\ldots,C} D(p_R\|p_{i,T}) \ . \tag{8}$$

Algorithm 1.

The multivariate Gaussian-based positioning method

Note: This is the main algorithm which corresponds to one spatial level (region) and one iteration. The region-based multivariate Gaussian approach extends it by performing it in a multi-level iterative fashion.

1. During training phase, collect RSSI measurements from APs at each cell *trainingAP(c)*: set of APs from which data are collected at cell c
2. During runtime, collect RSSI measurements from each AP at the unknown position *runtimeAPs*: set of APs from which data are collected *effectiveAP*(c): *trainingAP*(c) $\cap$ *runtimeAP*
3. During runtime, perform the following steps for each cell c:
   - Generate the training signature for cell c using only training measurements collected from APs $\in$ effectiveAP(c) (*i.e., training signature(c)*)
   - Generate the runtime signature using only runtime measurements collected from APs $\in$ effectiveAP(c) (*i.e., runtime signature(c)*)
   - Estimate the KLD distance of the training and runtime signatures
4. Report the cell c^* with the smallest KLD distance as the estimated position

2.4.1. An iterative multi-layer spatial aggregation of fingerprints

To improve the accuracy, we propose a generalization of the approach presented in Algorithm 1: instead of applying the multivariate Gaussian *per cell*, we apply it in an iterative fashion in multiple spatial levels (*e.g., regions*). First the physical space is divided into overlapping regions of equal size and the multivariate Gaussian algorithm is applied for each region separately. To generate the fingerprint of a region, we employ all the signal-strength measurements from all APs collected at positions within that region. This *spatial aggregation* reduces the likelihood of selecting a false region/cell (a region/cell that does not include/correspond to the actual position) over the correct one. Essentially, via this aggregation, it is likely that an incorrect region will be eliminated (in the first iteration), while the "weight" of the correct region will be enhanced by considering the signatures of the neighboring to the actual position cells. The *region-based multivariate Gaussian* algorithm proceeds iteratively: after it estimates the region at which the device is located, it repeats the process by dividing the selected region into sub-regions and applying the algorithm on them. This paper considers only two spatial levels: (i) at the top level, a grid representation of the entire physical space with coarse granularity is considered, with the entire area being divided into regions and (ii) at the second level, a finer granularity grid is adopted, with each region being divided into cells.

The physical space of interest is discretized in G regions, each of N cells. Let A_i be a $GK \times N$ matrix whose jth column ($\in \mathbb{R}^{GK}$) contains the received signal-strength values from the jth AP collected at cells of region i during training.

Let us denote with $A_{i,T}\left(\mathbf{x}|\boldsymbol{\mu}^s_{i,T}, \boldsymbol{\Sigma}^s_{i,\ T}\right)$ the multivariate Gaussian density of region i and $p_R(\mathbf{x}|\boldsymbol{\mu}^s_R, \boldsymbol{\Sigma}^s_R)$ the multivariate Gaussian density of the unknown position (runtime signature). The KLD distance can be computed as in (7) and the region closest to the unknown position is given by

$$i^*_A = \arg\min_{i=1,\ldots,G} D(p_R \| A_{i,T}). \tag{9}$$

After the estimation of the correct region, the process is repeated (using Algorithm 1) to compute the cell in that region that corresponds to the unknown position, considering only the cells of that region.

3. Compressive sensing WLAN localization

Let us first describe the main theoretical concepts of CS as applied in the context of positioning. Let $\mathbf{x} \in \mathbb{R}^N$ denote the signal of interest, that is, a vector of RSSI measurements. The efficiency of a CS method for signal approximation or reconstruction depends highly on the sparsity structure of the signal in a suitable transform domain associated with an appropriate sparsifying basis $\boldsymbol{\Psi} \in \mathbb{R}^{N\times D}$. It has been demonstrated [24,25] that if $\mathbf{x}$ is K-sparse in $\boldsymbol{\Psi}$ (meaning that the signal is exactly or approximately represented by K elements of this basis), it can be reconstructed from $M = rK \ll N$ non-adaptive linear projections onto a second measurement basis, which is incoherent[1] with the sparsity basis, and where r is a small overmeasuring factor ($r > 1$). For instance, in standard signal processing applications, several natural signals are often sparse in a discrete cosine transform (DCT) or in a Fourier basis.

The measurement model in the original space-domain is expressed as follows,

$$\mathbf{g} = \boldsymbol{\Phi}\mathbf{x}, \tag{10}$$

where $\mathbf{g} \in \mathbb{R}^M$ is the measurement vector and $\boldsymbol{\Phi} \in \mathbb{R}^{M\times N}$ denotes the measurement matrix. By noting that $\mathbf{x}$ can be expressed in terms of the basis $\boldsymbol{\Psi}$ as $\mathbf{x} = \boldsymbol{\Psi}\mathbf{w}$, where $\mathbf{w} \in \mathbb{R}^D$ denotes the vector of transform coefficients, the measurement model has the following equivalent transform-domain representation

$$\mathbf{g} = \boldsymbol{\Phi}\boldsymbol{\Psi}\mathbf{w}. \tag{11}$$

Examples of measurement matrices $\boldsymbol{\Phi}$, which are incoherent with any fixed transform basis $\boldsymbol{\Psi}$ with high probability (universality property [25]), are random matrices with independent and identically distributed (i.i.d.) Gaussian or Bernoulli entries. Since the original vectors of RSSI measurements, $\mathbf{x}$, are not sparse in general, in the following study we focus on the more general case of reconstructing their equivalent sparse representations, $\mathbf{w}$, given a low-dimensional set of measurements $\mathbf{g}$ and the measurement matrix $\boldsymbol{\Phi}$. The inherent sparsity in the problem of location estimation comes from the fact that the device to be localized can be placed in exactly one of the C non-overlapping cells. Let $\mathbf{w} = [0\ 0\ \cdots\ 0\ 1\ 0\ \cdots\ 0]^T \in \mathbb{R}^C$ be an indicator vector with its jth component being equal to "1" if the device is located in the jth cell. Thus, in the framework of CS, the problem of estimating the location of a mobile device is reduced to a problem of recovering the one-sparse vector $\mathbf{w}$. Of course in practice we do not expect an exact sparsity, thus, the estimated position corresponds simply to the largest-amplitude component of $\mathbf{w}$.

By employing the M compressive measurements and given the K-sparsity property in basis $\boldsymbol{\Psi}$, the sparse vector $\mathbf{w}$, and consequently the original signal $\mathbf{x}$, can be recovered perfectly with high probability by taking a number of different approaches. In the case of noiseless CS measurements the sparse vector $\mathbf{w}$ is estimated by solving a constrained ℓ_0-norm optimization problem of the form,

$$\hat{\mathbf{w}} = \arg\min_{\mathbf{w}} \|\mathbf{w}\|_0,\ s.t.\ \mathbf{g} = \boldsymbol{\Phi}\boldsymbol{\Psi}\mathbf{w}, \tag{12}$$

where $\|\mathbf{w}\|_0$ denotes the ℓ_0 norm of the vector $\mathbf{w}$, which is defined as the number of its non-zero components. However, it has been proven that this is an NP-complete problem, and the optimization problem can be solved in practice by means of a relaxation process that replaces the ℓ_0 with the ℓ_1 norm,

$$\hat{\mathbf{w}} = \arg\min_{\mathbf{w}} \|\mathbf{w}\|_1,\ s.t.\ \mathbf{g} = \boldsymbol{\Phi}\boldsymbol{\Psi}\mathbf{w}. \tag{13}$$

In [24,25] it was shown that these two problems are equivalent when certain conditions are satisfied by the two matrices $\boldsymbol{\Phi}$, $\boldsymbol{\Psi}$ (restricted isometry property (RIP)). In the later case, the sparse vector $\mathbf{w}$ can be recovered using $M \gtrsim K \cdot \log D$ CS measurements.

The objective function and the constraint in (13) can be combined into a single objective function, and several of

[1] Two bases $\boldsymbol{\Psi}_1$, $\boldsymbol{\Psi}_2$ are incoherent if the elements of the first are not represented sparsely by the elements of the second, and vice versa.

the most commonly used CS reconstruction methods solve the following problem,

$$\hat{\mathbf{w}} = \arg\min_{\mathbf{w}} (\|\mathbf{w}\|_1 + \tau\|\mathbf{g} - \mathbf{\Phi\Psi w}\|_2), \quad (14)$$

where τ is a regularization factor that controls the trade-off between the achieved sparsity (first term in (14)) and the reconstruction error (second term). Commonly used algorithms are based on linear programming [28], convex relaxation [24,29], and greedy strategies (*e.g.,* Orthogonal Matching Pursuit (OMP) [30,31]).

As it was mentioned before, a common characteristic of all RSSI-based fingerprint methods is their implementation in two distinct phases, namely, a *training phase* (off-line), and a *runtime phase* (on-line). In the following two subsections, the several requirements of each phase are described in detail. Besides, for convenience the following notations are used in the subsequent derivations: i) y_T denotes any quantity y that is related with the training phase, ii) y_R denotes that y is associated with the runtime phase.

3.1. Training phase specifications

During the training phase, a set of RSSI samples is collected at each cell from each AP. Let $\mathbf{x}_{j,T}^{i} \in \mathbb{R}^{n_{j,i}}$ denote the vector of training RSSI measurements received at cell j from AP i. In general $n_{j,i} \neq n_{j',i'}$ for $j \neq j'$, $i \neq i'$. To compensate for the potentially different number of RSSI measurements from cell to cell we set $N_i = \min_j\{n_{j,i}\}$, $i = 1, \ldots, P$, $j = 1, \ldots, C$. These vectors are generated for all cells by a central server, which forms a single matrix $\mathbf{\Psi}_T^i \in \mathbb{R}^{N_i \times C}$ for the ith AP by concatenating the corresponding C vectors. Then, this matrix is used as the appropriate sparsifying dictionary for the ith AP, since in the ideal case the vector of RSSI measurements at a given cell j received from AP i should be closer to the corresponding vectors of its neighboring cells, and thus it could be expressed as a linear combination of a small subset of the columns of $\mathbf{\Psi}_T^i$. Moreover, a measurement matrix $\mathbf{\Phi}_T^i \in \mathbb{R}^{M_i \times N_i}$ is associated with each transform matrix $\mathbf{\Psi}_T^i$, where M_i is the number of CS measurements. In the proposed algorithm, a standard Gaussian measurement matrix is employed, with its columns being normalized to unit ℓ_2 norm.

3.2. Runtime phase specifications

A similar process is followed during the runtime phase. More specifically, let $\mathbf{x}_{c,R}^{i} \in \mathbb{R}^{n_{c,i}}$ be the RSSI measurements received at the current unknown cell c from the ith AP. Notice that, since the acquisition time interval during the runtime phase is smaller than that in the training phase, it holds that $n_{c,i} < n'_{c,i}$, where $n'_{c,i}$ denotes the length of the corresponding RSSI vector generated at the same cell during the training phase. The runtime CS measurement model associated with the cell c and AP i is written as

$$\mathbf{g}_{c,i} = \mathbf{\Phi}_R^i \mathbf{x}_{c,R}^i, \quad (15)$$

where $\mathbf{\Phi}_R^i \in \mathbb{R}^{M_{c,i} \times n_{c,i}}$ denotes the corresponding measurement matrix during the runtime phase.

In order to overcome the problem of the difference in dimensionality between the training and runtime phase, while maintaining the robustness of the reconstruction procedure, we select $\mathbf{\Phi}_R^i$ to be a subset of $\mathbf{\Phi}_T^i$ with an appropriate number of rows such as to maintain equal measurement ratios, $\frac{M_i}{N_i} = \frac{M_{c,i}}{n_{c,i}}$. The measurement vector $\mathbf{g}_{c,i}$ is formed for each AP i according to (15) and transmitted to the server, where the reconstruction takes place via the solution of (14), with the training matrix $\mathbf{\Psi}_T^i$ being used as the appropriate sparsifying dictionary. We emphasize at this point the significant conservation of the processing and bandwidth resources of the wireless device by computing only low-dimensional matrix–vector products to form $\mathbf{g}_{c,i}$ ($i = 1, \ldots, P$) and then transmitting a highly reduced amount of data ($M_{c,i} \ll n_{c,i}$). Then, the CS reconstruction can be performed remotely (*e.g.*, at a server) for each AP independently. The final location estimate is the centroid of the estimated cells.

Finally, the overall CS-based localization method is summarized in Algorithm 2, while Table 1 gathers the symbols used in the CS setup. Here, we assume that the CS-based positioning method involves the mobile device (client) that collects the RSSI measurements from the beacons sent from the APs of the wireless infrastructure and a server that performs the core CS algorithm. The performance analysis (described in Section 4) reveals an increased accuracy of the proposed CS-based localization algorithm when compared with the statistical localization methods introduced in the previous sections.

Algorithm 2.

The compressive sensing positioning method

1. Training phase: collect RSSI measurements from all APs at each cell For each AP i, generate $\mathbf{\Phi}_T^i$ and $\mathbf{\Psi}_T^i$
2. Runtime phase: collect RSSI measurements from each AP at the unknown position For each AP i, generate $\mathbf{x}_{c,R}^i$
3. At runtime perform the following steps:
   - Send the length of runtime RSSI measurements, $n_{c,i}$, to the server
   - From each $\mathbf{\Phi}_T^i$, extract the columns until line $n_{c,i}$ and send it to the wireless device
   - Compute the measurements vector $\mathbf{g}_{c,i}$ and send it to the server
   - Perform CS reconstruction at the server by solving (14)
4. Report the centroid of the individual estimates given by the CS reconstruction scheme per AP c^* as the estimated position

4. Performance analysis

The following two subsections evaluate the performance of the proposed algorithms in two distinct real-world environments. As described, the training signatures are generated based on the collected signal-strength measurements at each cell of the two grid-based representations of the environments. In both cases, runtime measurements were collected at 35 randomly selected cells. The trainer (user) remained still for approximately 60 s (30 s) to collect beacons

Table 1
CS-WLAN symbols and notation.

P	Number of APs
C	Number of cells
$\mathbf{x}^i_{j,T}$, $\mathbf{x}^i_{j,R}$	Training/runtime RSSI set of measurements collected at cell j From the beacons sent by AP i
$n_{j,i}$	Number of RSSI measurements at cell j from AP i
$N_i = \min_j\{n_{j,i}\}$	Number of RSSI measurements kept at all cells for AP i
M_i	Number of CS measurements generated for AP i
$\mathbf{g}_{j,i}$	CS measurement vector at cell j for AP i
$\mathbf{\Phi}^i_T$, $\mathbf{\Phi}^i_R$	Training/runtime measurement matrix for AP i
$\mathbf{\Psi}^i_T$	Sparsifying matrix (dictionary) for AP i
$\mathbf{w}$	PSosition indicator (sparse) vector

at each position during training (runtime), respectively. This resulted in more than 100 and 200 RSSI values per AP at each cell for the runtime and training phases, respectively. To capture signal-strength values, *iwlist*, which polls each channel and acquires the MAC address and RSSI measurements from each AP (in dBm), and *tcpdump*, a packet analyzer relying on *libpcap*, were employed. A Sony Vaio and a Toshiba laptop with the same wireless adapter (ipw2200) were used for the collection of training and runtime signal-strength values. In the subsequent experiments, we evaluated our algorithms under the presence of different number of people. Let "Sc-A" and "Sc-B" denote the scenario corresponding to the presence of a small and a large number of people, respectively. We also note that in the subsequent evaluations, the MvG approach corresponds to the region-based implementation.

4.1. Evaluation at FORTH

The evaluation at FORTH took place in an area of 7 m × 12 m at TNL, which was discretized in a grid structure with cells of 55 cm × 55 cm. During the runtime phase two datasets are collected corresponding to the two scenarios: (i) Sc-A: the dataset was collected on a Sunday afternoon, with only one person, apart from the one collecting the measurements, present in the TNL (ii) Sc-B: the dataset was collected on a typical weekday late afternoon, during which there were from ten to fifteen people in the laboratory, and several others walking in the hallways outside. The training set included measurements from 84 different cells and was collected at the same period as the Sc-A runtime set. It was used both in the Sc-A and Sc-B scenarios. The total number of APs covering the area was 10, while on average 5.4 APs could be detected at a given cell.

In order to evaluate the performance of the various fingerprinting methods, we computed the *localization error*, measured as the Euclidean distance between the centers of the reported cell and the cell at which the mobile user was actually located at runtime. Note that the cell size affects the accuracy of the algorithms.

Fig. 2a and b presents the localization error of the different signature-based approaches during the Sc-A and the Sc-B scenario, respectively. As shown, the multivariate Gaussian model (MvG) outperforms the percentiles, the confidence interval (95%), and the empirical distribution approaches. More specifically, for the Sc-A dataset, the median error is equal to 2.19 m and 1.10 m for the confidence interval and percentiles, respectively, while the MvGs results in an error of 1.09 m. In Sc-B, the median error of the MvGs is 1.10 m, while the confidence interval (95%) and the percentiles methods report an error of 2.60 m and 2.20 m, respectively.

It is expected that as the number of APs that participate in the signature generation increases, so does the accuracy of distinguishing the correct cell from other further-away cells. To measure the impact of the number of APs on the accuracy, we associate each AP with a *popularity index* that indicates the number of cells at which measurements from the beacons of that AP were collected during both training and runtime phases. Let $|\{c|AP\ i \in effectiveAP(c)\}|$ denote the popularity index of AP i. The APs were sorted in a descending order based on their popularity indices and the analysis was repeated using the top k most popular APs for the Sc-A and Sc-B datasets. Fig. 3 shows the average localization error for the MvG algorithm as a function of the number of APs from which the RSSI measurements are employed. The larger the number of APs, the smaller the localization error. Interestingly, the effect of an increasing number of APs diminishes after a certain threshold. The number of APs affects more the performance of the MvG algorithm during the Sc-B than the Sc-A scenario.

Fig. 4a and b shows the localization accuracy as a function of the number of RSSI measurements for the MvG method. The % indicates the percentage of RSSI measurements considered in both the training and runtime datasets. We observe that the larger the measurement set, the more accurate the position estimation, since the statistical signature (mean and covariance) associated with the MvG method is estimated with a higher accuracy. Moreover, the increase in the number of RSSI measurements affects more the performance in the Sc-B scenario, where the environment is more dynamic with the presence of an increased number of people.

Finally, we comparatively analyze the performance of the CS-based localization and the MvG-based one. For this purpose, the CS reconstruction problem (14) is solved using a primal–dual interior point method (L1) and the orthogonal matching pursuit (OMP) algorithm[2].

Both CS methods employ only the 25% of the total runtime RSSI measurements. Fig. 5a and b shows the corresponding cumulative probability distributions of the localization error for the three methods. In particular, the median error for the Sc-A scenario is equal to 1.09 m for the MvG, and 1.08 m for the L1 and OMP approaches. Similar results are obtained for the Sc-B scenario with a median error of 1.09 m for the MvG and 1.08 m for the L1 and OMP methods. The similarity in performance in the case of TNL can be attributed to the simple topology of the indoor space and the relative position of the APs with respect to the people which were present in the lab, that did not affect significantly the variability of the RSSI measurements between the two scenarios.

[2] http://www.acm.caltech.edu/l1magic/, http://sparselab.stanford.edu/.

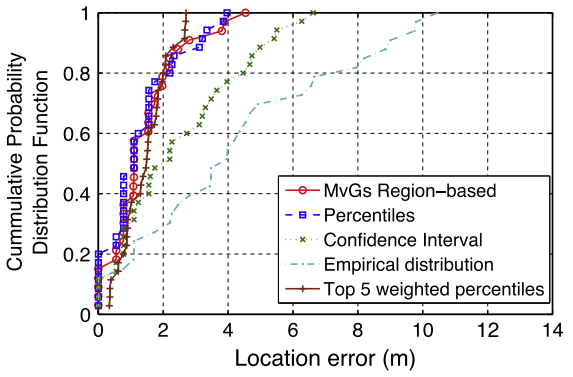

(a) Sc-A dataset

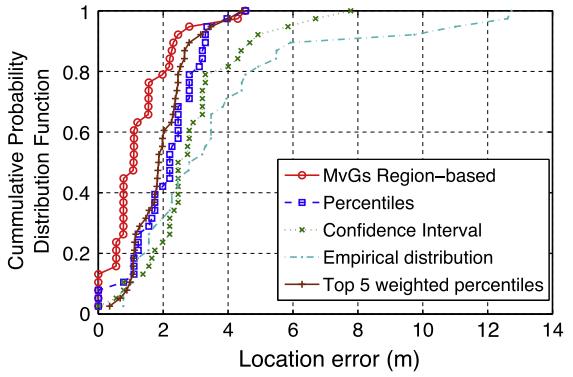

(b) Sc-B dataset

Fig. 2. Accuracy of various fingerprint positioning methods at FORTH.

Note an important difference on how the different algorithms employ the estimations per AP into the reported estimated position: The CS-based approach is carried out for each AP separately, using the compressed RSSI measurements, and the final estimate is given by the centroid of the individual estimated positions. On the other hand, the confidence interval, percentiles and empirical distribution methods perform an averaging over all APs of the values of the corresponding distance function *before* the final location estimation. For instance, in the case of the empirical distribution method, each cell is assigned a weight which corresponds to the average empirical KLD of each AP (at that cell) from the runtime measurements collected at the unknown position from the same AP. As a result, two cells with different KLD values between the individual APs may be reported erroneously to be close to each other after taking the average KLD, since the averaging operator eliminates the distinct contribution of each separate AP. This is not the case for a CS-based approach, where a "wrong estimation" based on a single AP can be "defused" if the estimates based on the remaining APs are close to the true cell.

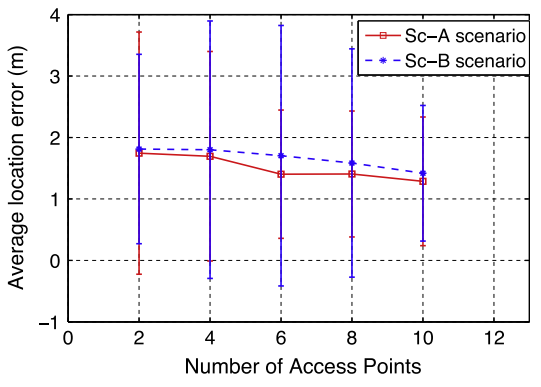

Fig. 3. Impact of the number of APs on localization error of the MvG method. The *x*-axis indicates the number of the top *x* APs considered in both training and runtime datasets.

4.2. Evaluation at the Cretaquarium

Cretaquarium is the largest and most popular aquarium in Greece, covering an area of 1760 m^2 and consisting of more than 40 tanks. The physical space was represented as a grid with cells of 1 m $\times$ 1 m. Seven IEEE802.11 APs were deployed, out of which 3.4 on average could be detected at a given cell. The training and runtime signal-strength measurements were collected in December, January and February of 2011 for the entire testbed under two different scenario conditions, with respect to the presence of visitors.

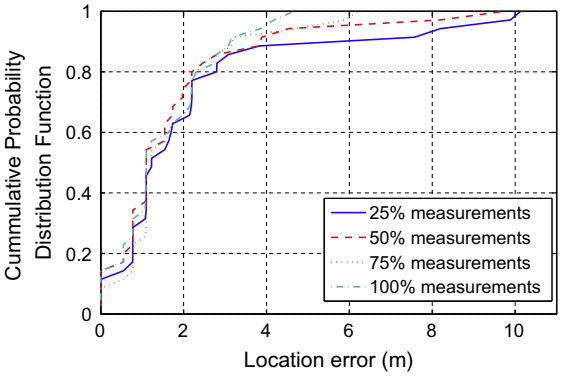

(a) Sc-A dataset

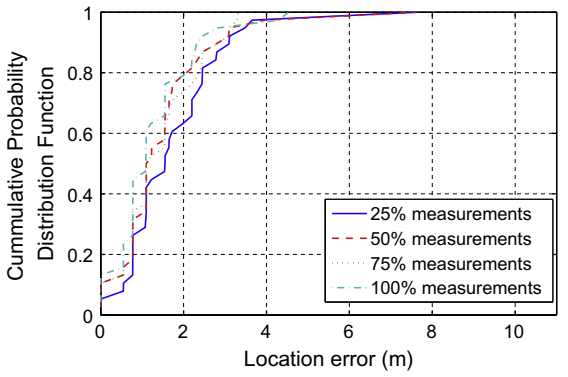

(b) Sc-B dataset

Fig. 4. Localization error as a function of the number of RSSI measurements for the MvG method.

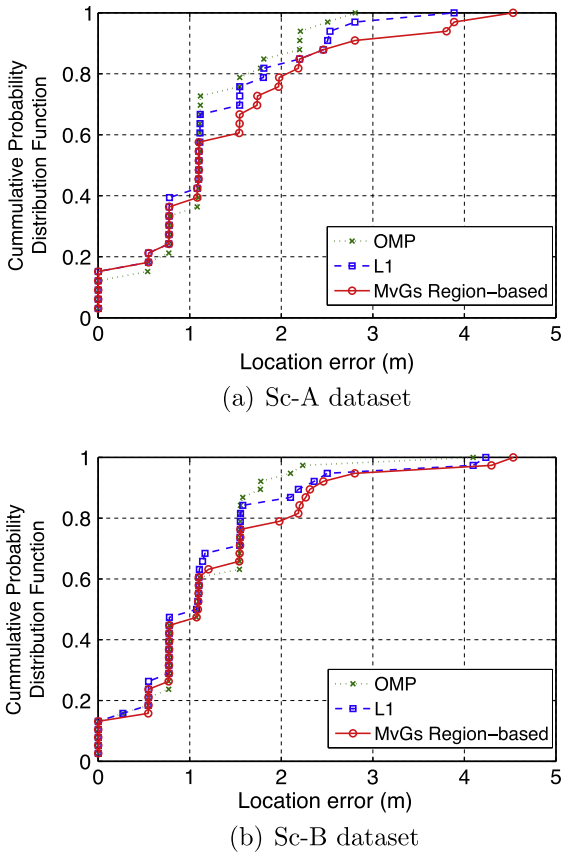

Fig. 5. Performance evaluation of the CS-based methods at FORTH.

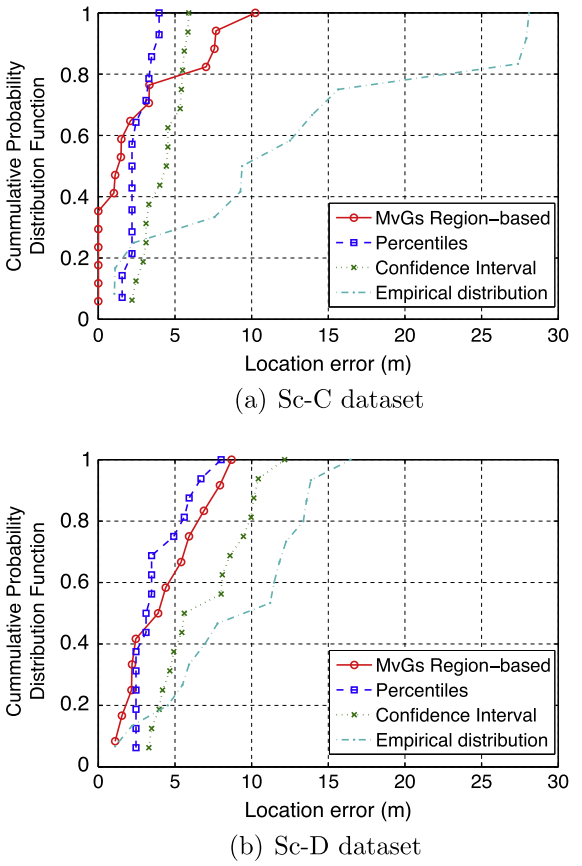

Fig. 6. Performance evaluation of various fingerprint positioning methods at Cretaquarium.

In the first set of measurements (*i.e.*, scenario Sc-C), there were only the two people that collected the signal-strength measurements present. During the collection of the second set of measurements (*i.e.*, scenario Sc-D), a group of students were visiting the Cretaquarium (with approximately 25 people near the trainers during that period).

Under the quiet conditions (Sc-C), the median localization error using the MvG method is 1.48 m, while the percentiles result in a median localization error of 2.20 m, as shown in Fig. 6a. Under the busier conditions (Sc-D), the median error of the percentiles method increases at 3.29 m, while the MvG results in an estimation error of 4.15 m (Fig. 6b). In both scenarios, the confidence intervals and the empirical distribution approaches exhibit significantly higher errors compared to the MvG method. As it was also the case for the experimental evaluation in the premises of TNL, the largest the measurement set, the more accurate the position estimation. Moreover, the large variance of the RSSI values affects more the estimation performance of the MvG method in the Sc-D scenario.

The presence of a large number of people, along with the complex topological layout of the Cretaquarium with its several tanks impose further challenges in the positioning. We compared the performance of the proposed CS-based localization technique with the MvG region-based one. As mentioned earlier, one of the advantages of a CS-based approach is its inherent ability to extract the salient information content of the signal by suppressing potential noise-like features. The complex topology of the Cretaquarium, as opposed to the simple topology of the TNL, and the particular conditions in the environment under which the experiments were performed cause the presence of such noise-like features.

As shown in Fig. 7a and b, for the Sc-C scenario the median error is equal to 1.48 m and 1.10 m for the MvG and the L1 method, respectively, while OMP results in a median error of 1.09 m. Besides, for the Sc-D scenario, the corresponding median error is equal to 4.15 m and 4.14 m for the MvG and the L1 method, respectively, while the OMP approach results in a median error of 3.59 m. The higher accuracy in the Sc-C scenario is due to the smaller variance of the RSSI measurements. As before, only 25% of the total runtime RSSI measurements were employed in the CS-based approach.

The proposed CS-based approach improves the localization accuracy compared to the MvG method in challenging environments, such as the Cretaquarium. This is because the CS-based scheme exploits directly the raw RSSI measurements, via the low-dimensional measurement vectors, and thus, it is able to take advantage of the full information content of the RSSI readings. On the other hand, the MvG method employs second-order RSSI statistics: it suppresses the RSSI measurements to their mean, variance and

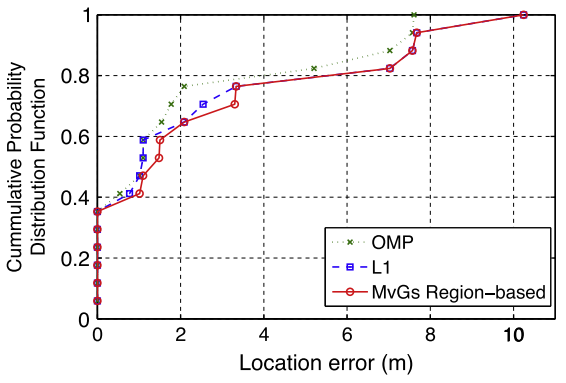

(a) Sc-C dataset

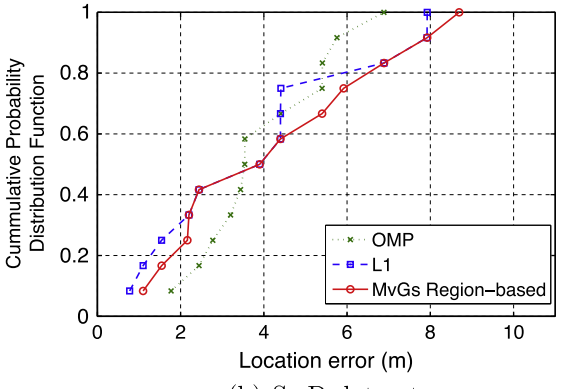

(b) Sc-D dataset

Fig. 7. Performance evaluation of CS-based methods at Cretaquarium.

covariance values. In addition, the CS approach suppresses the noise-like features of the signal to be reconstructed, but at the same time, it extracts its prominent information content. This is not the case with the MvG method, where the potential noise-like fluctuations in RSSI measurements may have a significant impact on the signatures, and consequently, on the computed KLD value. The ability to suppress the noise-like features, that may adversely affect the performance of a positioning algorithm, is important, since often positioning algorithms use explicitly or implicitly large-scale radio propagation (path-loss) attenuation models to estimate distances. A few very low RSSI values ("outliers") are often caused by small-scale transient phenomena in radio propagation. This observation enforces the need for a proper preprocessing of the RSSI measurements before their statistical analysis.

Moreover, the experimental evaluation using the collected data from two distinct environments shows that apart from the sparsifying basis $\mathbf{\Psi}$ and the measurement matrix $\mathbf{\Phi}$, the reconstruction algorithm that will be used can affect significantly the accuracy of the localization. For the present experimental configurations in the TNL and Cretaquarium, the OMP algorithm is an appropriate choice. However, one of the advantages of the CS framework is that the generation of CS measurements is fully decoupled with the process of reconstructing the corresponding sparse vector, that is, with the same set of CS measurements $\mathbf{g}$, the localization performance can be improved by developing a more efficient reconstruction technique.

5. Related work

Significant work has been published in the area of location-sensing using RF signals. Radar [2] employs signal-strength maps that integrate signal-strength measurements acquired during the training phase from APs at different positions with the physical coordinates of each position. Each measured signal-strength vector is compared against the reference map and the coordinates of the best match will be reported as the estimated position. Bahl et al. [32] improved Radar to alleviate side effects that are inherent properties of the signal-strength nature, such as aliasing and multipath. Ladd et al. [14] proposed another location-sensing algorithm that utilizes the IEEE802.11 infrastructure. In its first step, a host employs a probabilistic model to compute the conditional probability of its location for a number of different locations, based on the received signal-strength measurements from nine APs. The second step exploits the limited maximum speed of mobile users to refine the results and reject solutions with a significant change in the location of the mobile host. Kung et al. [33] proposed a method for evaluating the impact of the IEEE802.11 APs on positioning in order to strengthen the role/contribution of a "good" AP while "de-emphasizing" the role of the "bad" APs. The "goodness" of an AP indicates the capability of that AP to estimate accurately its distance from the others. Youssef's et al. Horus [15] substantially improved the accuracy (*e.g.,* an 1.3 m error in 90% of their experiments) by employing an autoregressive model that captures the autocorrelation in signal strength measurements of the same AP at a particular location. Specifically, the time series generated from signal-strength measurements collected from an AP is represented by a first-order autoregressive model. The fingerprints are formed for each cell and AP based on the degree of autocorrelation, the mean, and the variance of the empirical measurements collected from that AP at that cell. Finally, fingerprints based on attributes that characterize the effects of multipath (*e.g.,* channel response) for detecting changes of the positions of wireless hosts were presented in [34,35].

Researchers have also explored the cooperation for performing positioning. Niculescu and Badri Nath [36] designed and evaluated a cooperative location-sensing system that uses specialized hardware for calculating the angle between two hosts in an ad hoc network. This can be done through antenna arrays or ultrasound receivers. Hosts gather data, estimate their position, and propagate them throughout the network. Previously, these authors [19] introduced a cooperative location-sensing system in which position information of landmarks is propagated towards hosts that are further away, while during this process, hosts may further enrich this information by determining their own location. A location-sensing system in ad hoc networks that does not use landmarks or GPS was discussed in [18]. The location-sensing systems presented in [17 and 37] were the closest to our earlier work on cooperative location sensing (CLS) and were compared in detail in [20].

Active Badge [38] uses diffuse infrared technology and requires each person to wear a small infrared badge that emits a globally unique identifier every ten seconds or on demand. A central server collects this data from fixed infrared sensors around the building, aggregates it and provides an application programming interface for using the data. The system suffers in the case of fluorescent lighting and direct sunlight, because of the spurious infrared emissions these light sources generate. A different approach, SmartFloor [39], employs a pressure sensor grid installed in all floors to determine presence information in a building without requiring users to wear tags or carry devices, albeit without being able to identify individuals.

Examples of localization systems that combine multiple technologies are UbiSense [40], Active Bats [41] and SurroundSense [13]. UbiSense can provide a high accuracy using a network of ultra wide band (UWB) sensors installed and connected into a building existing network. The UWB sensors use Ethernet for timing and synchronization. They detect and react to the position of tags based on time difference of arrival and angle of arrival. An RF tag is a silicon chip that emits an electronic signal in the presence of the energy field created by a reader device in proximity. Location can be deduced by considering the last reader to see the card. RFID proximity cards are in widespread use, especially in access control systems. The Active Bats architecture consists of a controller that sends a radio signal and a synchronized reset signal simultaneously to the ceiling sensors using a wired serial network. Bats respond to the radio request with an ultrasonic beacon. Ceiling sensors measure time-of-flight from a reset to an ultrasonic pulse. Active Bat applies statistical pruning to eliminate erroneous sensor measurements caused by a sensor hearing a reflected pulse instead of one that travelled along the direct path from the Bat to the sensor. A relatively dense deployment of ultrasound sensors in the ceiling can provide within 9 cm of the true position for 95 % of the measurements. SurroundSense runs on a mobile phone to provide logical localization by generating fingerprints using sound, accelerometers, cameras and IEEE802.11. Tesoriero et al. [42] propose a passive RFID-based indoor location system that is able to accurately locate autonomous entities, such as robots and people, within a physical-space. Yang et al. [43] present an integrated framework for location estimation and action prediction, that combines two areas of interest, namely, location estimation and plan recognition. Working in this framework, action and plan recognition are carried out from low-level signals and location estimation, by employing an appropriate set of APs.

Ariadne [44] is an automated location determination system. It uses a two dimensional construction floor plan and only a single actual strength measurement. It generates an estimated signal strength map comparable to those generated manually by actual measurements. Given the signal measurements for a mobile, a proposed clustering algorithm searches that signal strength map to determine the current location of the mobile device.

In a recent work [45], the problem of indoor location estimation was also treated in a probabilistic framework. In particular, a reduced number of locations sampled to construct a radio map is employed in conjunction with an interpolation method, which is developed to effectively patch the radio map. Furthermore, a Hidden Markov Model (HMM) that exploits the user traces to compensate for the loss of accuracy is employed to achieve further improvement of the radio map due to motion constraints, which could confine possible location changes. Both the proposed multivariate Gaussian model-based algorithm and the HMM-based approach belong to the class of the probabilistic localization techniques. Usually, a probabilistic localization method is characterized by an increased performance when compared with a deterministic one, since it provides not only a point estimate of the user's position but also gives a confidence interval for the quality of this estimate. This can be used to improve further the estimation accuracy with the goal of reducing the uncertainty. However, a first key observation is the highly reduced complexity of our method compared to the HMM-based approach. In particular, it is a one-iteration method, where in each iteration only the simple estimate of a mean vector, a covariance matrix, and the computation of the Kullback–Leibler divergence between multivariate Gaussians (given in closed form) are required. On the other hand, the HMM-based localization technique requires several iterations to converge, while in each iteration several model parameters have to be estimated (approximately of the same dimensions as the parameters of our proposed method). However, the reduced computational complexity of the Gaussian-based technique comes at the cost of a potentially degraded location estimate under certain circumstances. For instance, in the case of "corrupted" measurements (*e.g.,* due to an AP failure or the presence of an obstacle), our method is much more sensitive, since it is based on measurements collected instantaneously. In contrast, the HMM-based approach could provide a more accurate estimate via the prior knowledge of a transition-probability matrix, which is preserved and re-estimated in each iteration in conjunction with the refinement achieved by an Expectation Maximization algorithm. In conclusion, the major benefit of our proposed algorithm, when compared with the HMM-based approach, is the significantly reduced computational complexity and implementation simplicity, as well as the high accuracy in several specific environments (obstacle-free, robust measurements) as it was revealed by the experimental evaluation. On the other hand, the HMM-based approach can be proved to be more robust in the case of system failures, but at the cost of requiring increased computational resources.

Although recent enough, the theory of CS has already motivated an increasing number of emerging applications in almost every signal processing field (http://dsp.rice.edu/cs). However, the development of CS-based localization methods using wireless LANs is still at an early stage. In [27,46], the location estimation algorithm is carried out on the mobile device by using the average RSSI values in order to construct the sparsifying basis $\mathbf{\Psi}$. Our proposed CS approach is applied directly on the raw RSSI measurements and not on their average as in [27,46], and thus, exploiting their time-varying behavior.

In a recent work [47], the problem of location estimation was treated in a framework that also takes advantage of the spatial sparsity. In particular, the location estimation

is formulated as a constrained ℓ_1-norm minimization problem based on a suitably learned dictionary. A signature is associated with each AP by averaging the RSSI measurements, which would be received by the AP from each potential cell of the discrete spatial domain. Then, the system builds the dictionary by concatenating the signatures from all APs. A similar signature is generated at the unknown runtime cell, which is then projected on the dictionary to form the vector of measurements. However, the lack of a random measurement matrix required when working in the framework of CS may decrease the system's robustness under unpredictable environmental conditions.

One of our recent related projects was the design and implementation of a guiding application that provides personalized information to visitors in an area. The application was integrated with a positioning system and was evaluated in the aquarium. For this purpose, the physical space was divided into 17 zones according to the application requirement. The positioning system reported the zone in which the visitor was located. Experiments were contacted using the Ekahau [4], a commercial positioning system, which also employs RSSI-based fingerprints. The tests took place at the same period and for the same runtime cells as in the Sc-D scenario described in Section 4.2, under a relatively large number of visitors walking close to the trainers. In each zone, the system was tested at three different positions. The correct zone was reported in 80% of the times, resulting in a median error of 4.6 m.

This paper builds on our earlier work on positioning [49,50,20].

6. Conclusions and future work

This paper introduced two novel localization methods based on RSSI measurements. In the first case, statistical signal-strength fingerprints are created using multivariate Gaussian distributions. The position of the device is estimated by computing the region with the training fingerprint that has the minimum KLD from the runtime fingerprint. In the second case, the localization problem was reduced in a sparse reconstruction problem in the framework of CS. The dimensionality of the original RSSI measurements was reduced significantly via random linear projections on a suitable measurement basis, while maintaining an increased localization accuracy.

The empirical evaluation revealed that the multivariate Gaussian method usually outperforms previous statistical signal-strength fingerprint approaches, while the CS-based approach achieved a superior performance when compared to the multivariate Gaussian-based technique. We performed an evaluation of various fingerprint methods in the premises of a research lab and an aquarium. The presence of people and the density and placement of APs have a prominent impact on the positioning accuracy. Furthermore, in the case of the multivariate Gaussian-based algorithm we experimented with a spatial multiscale iterative approach in which we applied the algorithm on larger regions to select the correct one, and then within the selected region to estimate the correct cell. Something similar was performed in the case of percentiles by selecting the top five candidate cells. We showed that it improves the accuracy by eliminating the distant incorrect cells and taking also into consideration the neighboring cells around the position of the user. In the context of the aquarium, mobility patterns can be formed and their integration in the localization system can further improve its accuracy.

We have been also experimenting with other modalities, such as infrared, cameras and QR codes to improve the location estimation. Specifically, in front of each landmark (*e.g.,* tank of the aquarium or office in the lab), a unique QR code can be placed along with three infrared sensors (*e.g.,* WII bar). The camera of the mobile device of a visitor may capture the QR code, recognize it, and thus identify the landmark, in front of which this visitor is standing [48]. Similarly, when the camera captures the infrared light from at least two infrared sources, it can estimate its distance from the landmark by measuring the distance of the two infrared sources on the recorded image. We plan to extend our localization system by incorporating these multi-modalities measurements.

There is a growing interest in statistical methods that exploit various spatio-temporal statistical properties of the received signal to form robust fingerprints. In general, a channel exhibits very transient phenomena and is highly time-varying. At the same time, the collection of signal measurements is subject to inaccuracies due to various issues, such as hardware misconfigurations, limitations, time synchronization, fine-grain data sampling, incomplete information, and vendor-specific dependencies (often not publicly available). A proper pre-processing of the RSSI measurements is required before applying the various statistical-analysis algorithms.

There are several potential extensions of the CS-based localization framework. In CS-based localization, the unknown location was estimated by performing separate reconstruction for each AP. A straightforward extension will be the use of the joint sparsity structure of the indicator vector $\mathbf{w}$ among the APs for the simultaneous location estimation. Moreover, the random nature of the measurement vectors associated with an RSSI vector could be exploited in order to enhance the encryption capabilities of the proposed CS localization approach, without the additional computational cost of a separate encryption protocol. The choice of appropriate sparsifying and measurement bases is crucial for an increased localization accuracy. The design of new transform and measurement bases that are adaptive to the specific characteristics of the RSSI data is also of significant importance. A new sparsifying basis being able to increase the degree of sparsity of an RSSI measurements vector, represented in terms of this basis, is critical in the framework of CS, since the reconstruction accuracy increases as the sparsity increases. Furthermore, an improved performance can be guaranteed with high probability by employing an appropriate measurement matrix, which is highly incoherent with the sparsifying basis.

Acknowledgments

This work was partially funded by the Marie Curie IAPP "CS-ORION" (PIAP-GA-2009-251605) grant within the 7th

Framework Program of the European Community and by the Greek General Secretariat for Research and Technology (Regional of Crete) Crete-Wise Grant.

References

[1] M. Youssef, A. Youssef, C. Rieger, U. Shankar, A. Agrawala, PinPoint: An asynchronous time-based location determination system, in: ACM MobiSys, Uppsala, Sweden, June 2006, pp. 165–176.
[2] P. Bahl, V. Radmanabhan, Radar: An in-building RF-based user location and tracking system, in: IEEE InfoCom, March 2000.
[3] Y. Gwon, R. Jain, T. Kawahara, Robust indoor location estimation of stationary and mobile users, in: IEEE InfoCom, Hong Kong, March 2004.
[4] Ekahau v.3.1. <http://www.ekahau.com>.
[5] R. Want, A. Hopper, V. Falcao, J. Gibbons, The active badge location system, ACM Trans. Info. Syst. 10 (1) (1992) 91–102.
[6] N.B. Priyantha, A. Chakraborty, H. Balakrishnan, The cricket location-support system, in: ACM MobiCom, August 2000.
[7] N.B. Priyantha, A. Miu, H. Balakrishnan, Teller, The cricket compass for context-aware mobile applications, in: ACM MobiCom, Rome, Italy, July 2001, pp. 1–14.
[8] U. Bandara, M. Hasegawa, M. Inoue, H. Morikawa, T. Aoyama, Design and implementation of a bluetooth signal strength based location sensing system, in: IEEE RAWCON, Atlanta, GA, USA, September 2004.
[9] S. Feldmann, K. Kyamakya, A. Zapater, Z. Lue, An indoor bluetooth-based positioning system: concept, implementation and experimental evaluation, in: Intern. Conf. on Wireless Networks, Las Vegas, Nevada, USA, 2003, pp. 109–113.
[10] M. Rodriguez, J.P. Pece, C.J. Escudero, In-building location using bluetooth, in: International Workshop on Wireless Ad-hoc Networks, Coruna, Spain, May 2005.
[11] S. Asthana, D. Kalofonos, The problem of bluetooth pollution and accelerating connectivity in bluetooth ad-hoc networks, in: IEEE PerCom, New York, NY, USA, 2005.
[12] A. Roy, A. Misra, S.K. Das, An information theoretic framework for optimal location tracking in multi-system 4G wireless networks, in: IEEE InfoCom, Hong Kong, March 2004.
[13] M. Azizyan, I. Constandache, R. Choudhury, SurroundSense: Mobile phone localization via ambience fingerprinting, in: ACM MobiCom, September 20–25, 2009.
[14] A. Ladd, K. Bekris, A. Rudys, G. Marceau, L. Kavraki, D. Wallach, Robotics-based location sensing using wireless Ethernet, in: ACM MobiCom, Atlanta, GE, USA, September 2002.
[15] M. Youssef, A. Agrawala, The horus WLAN location determination system, in: ACM MobiSys, June 6–8, 2005.
[16] K. Vandikas, L. Kriara, T. Papakonstantinou, A. Katranidou, H. Baltzakis, M. Papadopouli, Empirical-based analysis of a cooperative location-sensing system, in: ACM First International Conference on Autonomic Comp. and Comm. Systems (Autonomics), Rome, Italy, October 2007.
[17] C. Savarese, J. Rabaey, K. Langendoen, Robust positioning algorithms for distributed ad-hoc wireless sensor networks, in: USENIX, Monterey, CA, June 2002.
[18] S. Capkun, M. Hamdi, J.-P. Hubaux, GPS-free positioning in mobile ad-hoc networks, in: Proc. Hawaii International Conference on System Sciences, Hawaii, January 2001.
[19] D. Niculescu, B. Nath, Ad hoc positioning system (APS), in: IEEE GlobeCom, San Antonio, TX, November 2001.
[20] C. Fretzagias, M. Papadopouli, Cooperative location sensing for wireless networks, in: IEEE PerCom, Orlando, Florida, March 2004.
[21] K. Chintalapudi, R. Govindan, G. Sukhatme, A. Dhariwal, Ad-hoc localization using ranging and sectoring, in: IEEE InfoCom, Hong Kong, March 2004.
[22] L. Fang, W. Du, P. Ning, A beacon-less location discovery scheme for wireless sensor networks, in: IEEE InfoCom, Miami, Florida, Mar. 2005, pp. 161–171.
[23] J. Hightower, G. Borriello, A survey and taxonomy of location sensing systems for ubiquitous computing, Tech. Rep., Univ. of Washington, Dept. of Computer Science and Engineering UW CSE 01-08-03, Seattle, WA, August 2001.
[24] E. Candés, J. Romberg, T. Tao, Robust uncertainty principles: exact signal reconstruction from highly incomplete frequency information, IEEE Trans. Inform. Theory 52 (2006) 489–509.
[25] D. Donoho, Compressive sensing, IEEE Trans. Inform. Theory 52 (4) (2006) 1289–1306.
[26] C. Feng, S. Valaee, Z. Tan, Multiple target localization using compressive sensing, in: Proceedings of IEEE GLOBECOM'09, Hawaii, USA, 4 November–5 December, 2009.
[27] C. Feng, W. Au, S. Valaee, Z. Tan, Compressive sensing based positioning using RSS of WLAN access points, in: Proc. IEEE INFOCOM'10, San Diego, CA, March 2010.
[28] S. Chen, D. Donoho, M. Saunders, Atomic decomposition by basis pursuit, SIAM J. Sci. Comp. 20 (1) (1999) 33–61.
[29] R. Tibshirani, Regression shrinkage and selection via the lasso, J. Roy. Stat. Soc. Ser. B (Methodol.) 58 (1) (1996) 267–288.
[30] J. Tropp, A. Gilbert, Signal recovery from random measurements via orthogonal matching pursuit, IEEE Trans. Inform. Theory 53 (2007) 4655–4666.
[31] D. Donoho, Y. Tsaig, I. Drori, J.-L. Starck, Sparse solution of underdetermined linear equations by stagewise orthogonal matching pursuit, Tech. Rep., Stanford, 2006 <http://www-stat.stanford.edu/donoho/Reports/2006/StOMP-20060403.pdf>.
[32] V. Paramvir Bahl, A. Balachandran, Enhancements to the radar user location and tracking system, Tech. Rep., Microsoft Research, February 2000.
[33] H. Kung, C.-K. Lin, T.-H. Lin, D. Vlah, Localization with snap-inducing shaped residuals (sisr): coping with errors in measurement, in: ACM MobiCom, September 20–25, 2009.
[34] N. Patwari, S. Kasera, Robust location distinction using temporal link signatures, in: ACM MobiCom, September 9–14 2007.
[35] J. Zhang, M. Firooz, N. Patwari, S. Kasera, Advancing wireless link signatures for location distinction, in: ACM MobiCom, September 14–19, 2008.
[36] D. Niculescu, B. Nath, Ad Hoc Positioning System (APS) using AoA, in: IEEE InfoCom, San Francisco, CA, April 2003.
[37] T. He, C. Huang, B. Blum, J. Stankovic, T. Abdelzaher, Range-free localization schemes for large-scale sensor networks, in: ACM MobiCom, San Diego, CA, USA, September 2003.
[38] R. Want, A. Hopper, Active badges and personal interactive computing objects, Tech. Rep. ORL 92-2, Olivetti Research also in IEEE Transactions on Consumer Electronics, February 1992.
[39] Future computing environments. <http://www.cc.gatech.edu/fce/smartfloor/>.
[40] Precise real-time location. <http://www.ubisense.net/>.
[41] The bat ultrasonic location system. <http://www.cl.cam.ac.uk/research/dtg/attarchive/bat/>.
[42] M. Tesoriero, R. Tebara, J. Gallud, M. Lozanoa, V. Penichet, Improving location awareness in indoor spaces using RFID technology, in: Expert System Application.
[43] Q. Yang, Y. Chen, J. Yin, X. Chai, LEAPS: A location estimation and action prediction system in a wireless LAN environment, in: Proceedings of Network and Parallel Computing, IFIP International Conference, NPC 2004, Wuhan, China, October 18–20, 2004, pp. 584–591.
[44] Y. Ji, S. Biaz, S. Pandey, P. Agrawal, Ariadne: A dynamic indoor signal map construction and localization system, in: ACM MobiSys, June 19–22, 2006.
[45] X. Chai, Q. Yang, Reducing the calibration effort for probabilistic indoor location estimation, in: IEEE Transactions on Mobile Computing, June 2007.
[46] C. Feng, W. Au, S. Valaee, Z. Tan, Orientation-aware indoor localization using affinity propagation and compressive sensing, in: Proceedings of IEEE CAMSAP'09, Dutch Antilles, December 2009.
[47] S. Nikitaki, P. Tsakalides, Localization in wireless networks via spatial sparsity, in: Proceedings of 44th ASILOMAR'10, Pacific Grove, CA, November 2010.
[48] A. Alexandridis, P. Charonyktakis, A. Makrogiannakis, A. Papakonstantinou, M. Papadopouli, Forthroid on Android: A QR-code based Information Access System for Smart Phones, in: Proceedings of IEEE LANMAN'11, Chapell Hill, North Carolina, USA, October 2011.
[49] D. Milioris, L. Kriara, A. Papakonstantinou, G. Tzagkarakis, P. Tsakalides, M. Papadopouli, Empirical evaluation of signal-strength fingerprint positioning in wireless LANs, in: Proceedings of 13th ACM International Conference on Modeling, Analysis and Simulation of Wireless and Mobile Systems, Bodrum, Turkey, October 2010.
[50] K. Vandikas, L. Kriara, T. Papakonstantinou, A. Katranidou, H. Baltzakis, M. Papadopouli, Empirical-based analysis of a cooperative location-sensing system, in: Proc. First International Conference on Autonomic Computing and Communication Systems (ACM Autonomics'07), Rome, Italy, October 2007.

Dimitrios Milioris received the B.S. degree in Computer Science from the University of Crete (UOC), Greece, in 2009 and a double M.Sc. degree (First in Class, Honors) in Computer Science from Paris XI University and University of Crete (2011). Since 2008 he has been a research assistant at the Telecommunications and Networks Laboratory (TNL) of the Foundation for Research and Technology-Hellas (FO.R.T.H.). In 2010 he joined Hipercom Team of the Institut National de Recherche en Informatique et en Automatique (I.N.R.I.A. – Rocquencourt campus) as a research assistant. His research interests lie in the field of signal processing, mobile computing, performance analysis, sensor networks, compressive sensing, indoor localization and information theory.

George Tzagkarakis received the B.S. degree in Mathematics from the University of Crete (UOC), Greece, in 2002 (First in Class, Honors). At the same year he joined the Computer Science department (CSD) at the UOC for graduate studies with scholarships from the CSD and the Institute of Computer Science (ICS) of the Foundation for Research and Technology-Hellas (FO.R.T.H.). He received the M.Sc. (First in Class, Honors) and the Ph.D. degrees from the CSD in 2004 and 2009, respectively. Since 2000, he has been also collaborating with the Wave Propagation Group of the Institute of Applied and Computational Mathematics (FO.R.T.H.), while from 2002 he is a research assistant in the Telecommunications and Networks Lab (ICS-TNL). Currently he is a post-doctoral researcher under a Marie Curie fellowship at CEA, Saclay (France). His research interests lie in the fields of statistical signal & image processing with emphasis in non-Gaussian heavy-tailed modeling, compressive sensing with applications in video processing, distributed signal processing for sensor networks, information theory, and inverse problems in underwater acoustics.

Artemis Papakonstantinou received a B.Sc. degree in Computer Science (2007) and a M.Sc. degree in Computer Science (2011), both from the Computer Science Department, University of Crete, Greece. Since 2008 she has been a research assistant at the Telecommunications and Networks Lab (TNL) of the Institute of Computer Science, Foundation for Research and Technology-Hellas (ICS-FORTH). Her research interests lie in the fields of wireless networks, mobile and pervasive computing with emphasis on location sensing and location based services (LBS), and smartphone applications and services.

Maria Papadopouli (Ph.D. Columbia University, October 2002) is a tenured assistant professor in the Department of Computer Science, University of Crete, a guest professor at the EE KTH Royal Institute of Technology, in Stockholm, and a research associate in FORTH-ICS. From July 2002 until June 2006, she was a tenure-track assistant professor at UNC (on leave from July 2004 until June 2006). Her current research interests are in wireless networking, modeling and performance analysis, network measurements, cognitive radio networks, mobile peer-to-peer computing, positioning, and pervasive computing. She has co-authored a monograph on Peer-to-Peer Computing for Mobile Networks: Information Discovery and Dissemination (Springer Eds. 2009). She has been the co-chair of nine international workshops in the area of wireless networks and mobile peer-to-peer computing and has given more than 25 invited talks in research labs and universities world-wide. In 2004 and 2005, she was awarded with an IBM Faculty Award.

Panagiotis Tsakalides received the Diploma in electrical engineering from the Aristotle University of Thessaloniki, Greece, in 1990, and the Ph.D. degree in electrical engineering from the University of Southern California (USC), Los Angeles, in 1995. He is a Professor of Computer Science at the University of Crete, and a Researcher with the Institute of Computer Science, Foundation for Research and Technology-Hellas (FORTH-ICS), Greece. From 2004 to 2006, he served as the Department Chairman. From 1999 to 2002, he was with the Department of Electrical Engineering, University of Patras, Patras, Greece. From 1996 to 1998, he was a Research Assistant Professor with the Signal and Image Processing Institute, USC, and he consulted for the US Navy and Air Force. His research interests lie in the field of statistical signal processing with emphasis in non-Gaussian estimation and detection theory, and applications in sensor networks, audio, imaging, and multimedia systems. He has coauthored over 100 technical publications in these areas, including 25 journal papers. He is the PI of the 1.3 M euros FP7 MC-IAPP "CS-ORION" project (2010–2014) conducting research on compressed sensing for remote imaging in aerial and terrestrial surveillance. He is a member of the ERCIM Network of Innovation/Technology and Knowledge Transfer Experts (I-Board).